IHJPAS. 37 (1) 2024
Ibn Al-Haitham Journal for Pure and Applied Sciences
Journal homepage: jih.uobaghdad.edu.iq
PISSN: 1609-4042. EISSN: 2521-3407

Synthesis and Study Medical Application of Nanocomposites Based on Grafted Chitosan /Polyvinyl Alcohol

[1]Widad Abed Shlaka [2]Ruwaidah Samir Saeed* [3]El-Sayed Negim

[1]Department of Chemistry, College of Science, Mustansiriyah University, Baghdad, Iraq.
[2]Department of Chemistry, College of Education for Pure Science Ibn Al-Haitham, University of Baghdad, Baghdad ,Iraq.
[3]School of Petroleum Engineering, Satbayev University, 22 Satpayev Street, Almaty 050013, Kazakhstan.

*Corresponding Author: ruaida.s.s@ihcoedu.uobaghdad.edu.iq

Received 12 March 2023, Received 16 April 2023, Accepted 2 May 2023, Published 20 January 2024

doi.org/10.30526/37.1.3327

Abstract

In the present study, synthesis of bis Schiff base [I, II] by reaction of one mole of terephthalaldehyde with two mole of 2-amino-5-mercapto-1,3,4-thiadiazole or 4-amino benzene thiol in the ethanol absolute, then compounds [I,II] were reacted with Na_2CO_3 of distilled H_2O, then chloroacetic acid was added to yield compounds [III,IV]. *O*-chitosan derivatives [V,VI] were synthesized by reaction of chitosan with compounds [III,IV] in acidic media in distilled water according to the steps of Fischer. *O*–chitosan (grafted chitosan) [V,VI] was blended with synthetic polymer polyvinyl alcohol (PVA) to produce polymers [VII,VIII], then these polymers were blended with nano: Gold or Silver by using a hotplate stirrer for 3 hours to produce nanocomposites [IX- XII]. The synthesized polymers were identified using spectral analysis techniques, including FTIR,^{1}H-NMR, and scanning electron microscope (SEM). Molecular docking was studied, where operations are used to predict the binding status of compounds with the enzyme and to calculate the free energy (ΔG) of the prepared compounds. Finally, the study of biological activities was screened via two types of bacteria. Also, the anti-cancer activity against human lung adenocarcinoma cells (A549) was studied and compared with standard cell line [REF(R7540) Rat Embryonic Fibroblasts] of some of the blended polymers and nanocomposites, then the acute toxicity test of some nanocomposites was performed.

Keywords: Rat embryonic fibroblasts, Nanocomposites, Molecular docking, Toxicity study, *O*-Chitosan

1. Introduction

Chitosan is produced from chitin found in the cell walls of fungi, the cuticles of insects, and the shells of mollusks and crustaceans [1]. Chitosan can be defined as a cationic linear polysaccharide made up of specific N-acetylglucosamine units and (β 1,4) linked glucosamine units [2]. Since

chitosan is unique in that it possesses qualities including biocompatibility, non-toxicity, anti-microbial activity, anticancer activity, and biodegradability, it could be employed effectively in a variety of biomedical applications [3,4]. The structure of chitosan is easy to modify to several derivatives due to -OH and NH_2 groups found [5], which distinct chitosan from cellulose [6].

The modified chitosan exhibits new properties such as solubility, biological activity [7], biocompatibility, and hydrophilicity [8]. Poly (vinyl alcohol) (PVA) can be defined as one of the synthetic polymers, which are mainly composed of C-C bonds [9,10]. It's non-toxic, water-soluble, biocompatible, and biodegradable, which makes it widely applicable in the biomedical field [11].

In the case of the PVA and the chitosan, their sufficient miscibility results from bonds of hydrogen that are formed between their functional groups [12,13]. Chitosan blend with PVA plays a role in receiving homogeneous materials that have anti-microbial characteristics and are more sufficient than Chitosan [14,15].

The biomedical field has paid close attention to gold nanoparticles (AuNPs), among other functional nanomaterials, because of their nontoxicity, biocompatibility, and ease of manufacture [16,17]. Additionally, silver nanoparticles (AgNPs) have been shown to have enough potential to treat cancer [18]. The physical, chemical, and biological properties of CS, when combined with AuNPs, AgNPs were widely utilized in various medicinal applications and drug delivery [19,20].

2. Materials and Methods

BDH and SCR supplied chemicals. The ^{1}H-NMR spectra were performed by the company Ultra Shield 500 MHz, Bruker, University of Tehran, Iran, and DMSO as solvent has been used-Shimadzu FT-IR-8400 s, with FT-IR spectra between 400 cm^{-1} and 4000 cm^{-1}. A fully licensed CCDC genetic optimization for ligand docking (GOLD) Hermes 2021.2.0 (Build 327809) was used to record the molecular docking studies for the compounds and visualize the protein, ligands, hydrogen bonding interactions, short contacts, and bonds length calculation. University of Tabriz, Iran, performed SEM.

2.1 Synthesis of 2-amino-5-mercapato-1,3,4-thiadiazole

According to the literature [21], this compound is prepared and gives a good yield of 87%, M.P. (229-231) Celsius.

2.2 Synthesis of compounds [I,II]

Terephthalaldehyde (1.34 g, 0.01 mol) mixed with (2.5 g, 0.02 mol) 4-amino benzene thiol or (2.66 g, 0.02 mol) 2- amino-5- mercapto -1,3,4 – thiadiazole, Ethanol absolute (20 mL), with two drops of glacial acetic acid, refluxing at 70 °C for 18h. The reaction mixture was cooled, and the yellow precipitate filtration was recrystallized from ethanol and dried to yield 80% and 95% [22].

2.3 Synthesis of compounds [III,IV]

One of the compounds (0.01 mol) [I, II] was mixed with (0.04 mol) Na_2CO_3 in (15 mL) of distilled H_2O, then (0.02 mol) of $ClCH_2COOH$ was added. The solution refluxed for six hours, then was added conc. HCl reached out PH= 2. then filtered and washed with H_2O and recrystallized by EtOH [23] **Scheme 1.**

2.4 Synthesis of *O*- chitosan derivatives [V,VI]

Chitosan (0.5 gm) was hanging in 25 mL of H_2SO_4 (2M) and added (0.01 mol) of compounds [II I, IV] to this solution. The mixture refluxed for eight hours before cooling. $NaHCO_3$ was used to neutralize the pH and keep it at 7. The product was precipitated in acetone, filtered, and then was hed with acetone to remove any remaining acid. It was then dried at 60 Celsius in an oven for 24 hours [24].

2.5 Synthesis of polymer blend [VII- VIII]

Polymer blends were produced by using the solvent casting method. The grafted chitosan [V, VI] solutions were dissolving [V, VI] in a 2% solution of aqueous acetic acid with stirring at room temperature. Polyvinyl alcohol (PVA) was dissolved in the hot water to produce five wt% polymer solutions. Both solutions of the polymers were mixed, and a homogenous solution was made using a hot-plate stirrer for 60 min. The Grafted Cs/PVA blends were done through the mixing of (one ratio) Grafted Cs: PVA (5:5) [25].

2.6 Synthesis of grafted Cs/ PVA /nanocomposites [IX- XII]

About 100 mg of the dried Grafted Cs/PVA blend [VII- VIII] was put in 50 mL of the Au or Ag solution of a 250 mg/L concentration by using a hotplate stirrer for (3 hr.) to bond the gold and silver nanometal in blend matrix [26].

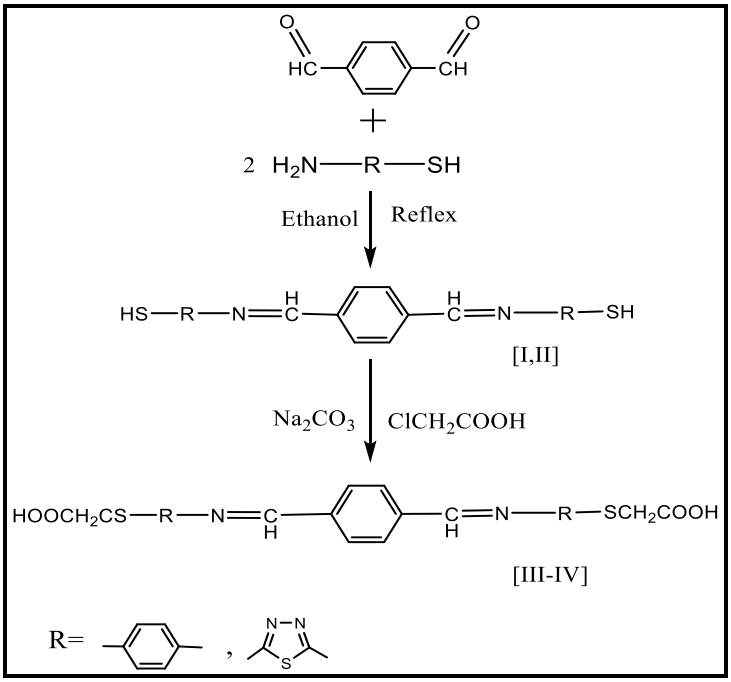

Scheme 1. Synthesis of compounds [I- IV]

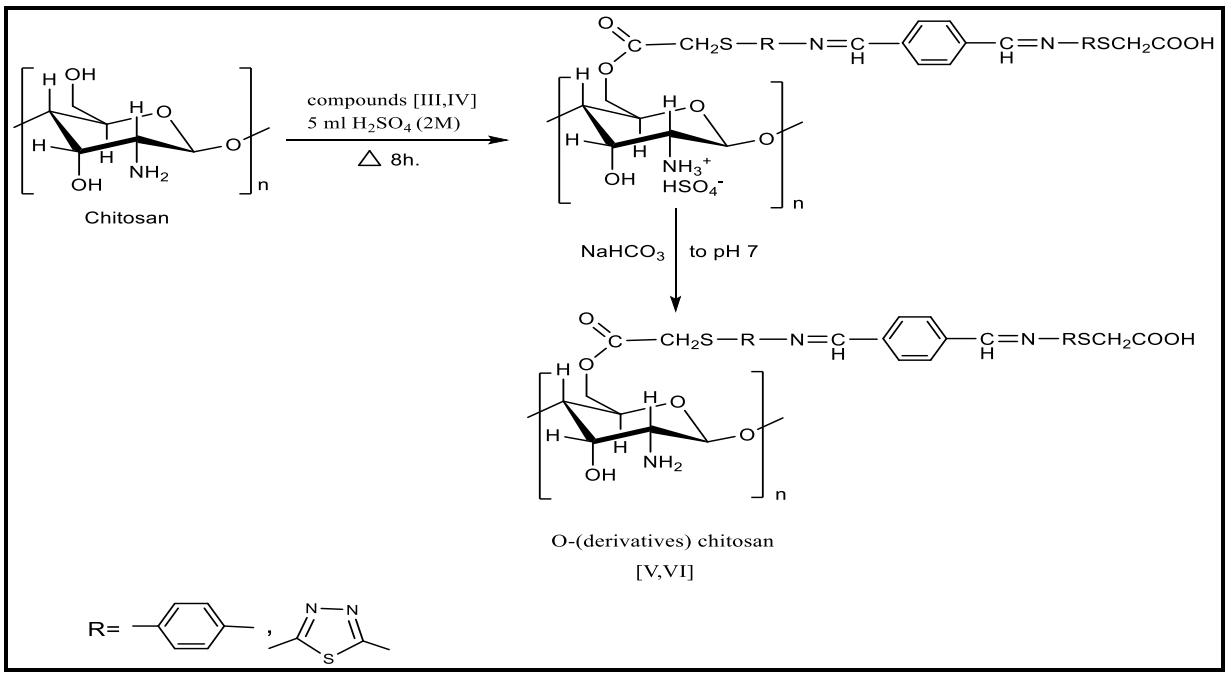

Scheme 2. Synthesis of *O*-Chitosan [V,VI]

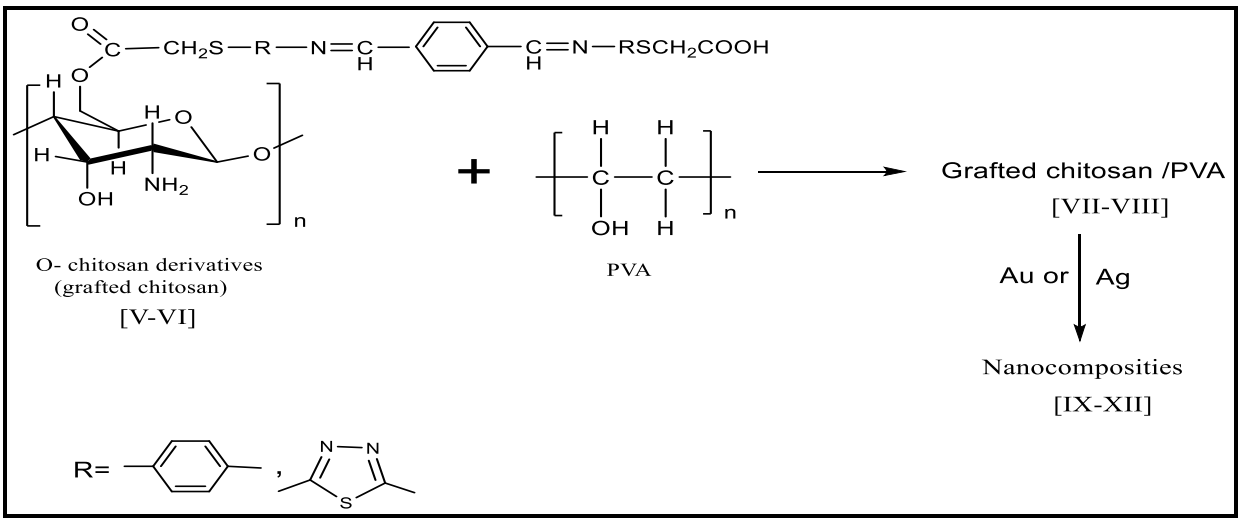

Scheme 3. Synthesis of blend polymers and nanocomposities [VII -XII]

3. Results and Discussion

3.1 The FTIR and ^{1}H-NMR of synthesis compounds, grafted chitosan and blend polymers

The synthesis of new derivatives started with bis Schiff bases is demonstrated in **Scheme 1.** Compounds [I, II] were created by reacting terephthalaldehyde with either 4-amino benzene thiol or 2-amino-5-mercapto-1,3,4-thiadiazole in ethanol at reflux for 18 hours. The compound's FT-IR [I] revealed appearance bands at (2547 and 1639) cm^{-1}, respectively, because of the SH group and (C=N) as shown in **Table1**. Compounds [III, IV] were prepared in primary media by the reaction compounds [I, II] with chloroacetic acid in distilled water. The FTIR spectrum of compound [III] in **Table 2** establishes a band at (3400-2400) cm^{-1} for the hydroxyl group and (1688) cm^{-1} for the carboxylic group. The ^{1}H-NMR exhibited a broad singlet signal with a chemical shift at δ 13.14 ppm as a result of the two protons of carboxylic protons; additional signal at δ10.07 ppm due to the presence of two protons for CH-N, multiple peaks appeared at δ(7.33-8.89) ppm for aromatic protons as well as a singlet signal at δ 3.91 for four protons for S-CH_2. The reaction between [III,

IV] and chitosan in distilled water in acidic media, Scheme (2), produced the new *O*-chitosan derivatives [V, VI]. The FT-IR of polymer [V] in **Table 3** interpreted with the existence of a large band at (3294) cm^{-1} as the stretch band regarding O-H as well as N-H from intra- and extra-molecular hydrogen bonding of chitosan molecules as well as a new absorption band at (1716) cm^{-1} due to ester's C=O. The ^{1}HNMR of polymer [V] elucidated a singlet signal with a chemical shift region at δ 12.75 ppm as a result of the proton of carboxylic protons (8.72-8.75) ppm due to the presence of protons of hydroxyl groups of chitosan, a multiple signals at δ(7.20-8.10) ppm for aromatic protons, singlet signal at δ7.98 ppm as a result of the presence of two protons for N-CH groups, singlet signal at δ6.53 ppm for proton of SCH_2 groups and signal at 5.84 ppm due to CH_2O, also the characteristic region at (3.42-4.32) ppm corresponded to the non-anomeric proton (H-1, H-3, H-4, H-5 and H-6) of chitosan, singlet signal at δ1.89 ppm for two protons of NH_2 group [27], a signal at 1.20 ppm assigned to H-2 and signal at 1.02 ppm existed because of the presence of CH_3 of N-alkylated of glucosamine residue. *O*-Chitosan derivative (Grafted chitosan) blended with PVA [VII- VIII] was prepared research of characteristics of obtained blends had shown a good level of the miscibility between the PVA and Chitosan that FT-IR results of the polymer had demonstrated [VII], the band broadening in (2400-3600) cm^{-1} region because of a solid inter-molecular bonding of hydrogen that exists between amino groups of Chitosan and PVA's hydroxyl groups, 1715 cm^{-1} which meaning C=O ester group.

Table 1. The FT-IR spectroscopy data of compounds [I,II]

Comp. No.	(S-H) cm^{-1}	=C-H arom.	(C=N)	(C=N) of thiadiazole	(C-S)
[I]	2547	3050	1639	-	696
[II]	2540	3081	1645	1613	700

Table 2. The FT-IR spectroscopy data of compounds [III,IV]

Comp. No.	(O-H)cm^{-1}	(C-H)arom. cm^{-1}	(C=O) carboxlic cm^{-1}	(C=N)	(C=C) cm^{-1}
[III]	3400-2400	3055	1688	-	1583
[IV]	3400-2400	3043	1690	1607	1595

Table 3. The FT-IR of grafted chitosan and blend polymers[[V-VIII]

Comp. No.	υ (O-H) and (N-H)	υ (C-H) aliph.	υ (C=O) ester.	υ (C=C)	υ (-CH_2-O-CO)	υ (C-O-C)
[V]	3294	2938, 2914	1716	1579	1371	1069
[VI]	3419	2943, 2872	1710	1590	1243	1048
[VII]	3274	2909, 2858	1715	1601	1271	1068
[VIII]	3269	2939, 2909	1703	1580	1240	1080

3.2 Molecular docking study

Molecular docking in **Table 4**, **Figure 1**, and **Figure 2** were studied, where operations are used to predict the binding status of compounds with the enzyme and to calculate the free energy (ΔG) of the compounds prepared with the enzyme 3-hydroxy-3-methylglutaryl-CoA reductase (HMGR), as well as the study of molecular similarity.

1DQ9: Mevalonate was produced due to 3-hydroxy-3-methylglutaryl-CoA reductase (HMGR), a committed step in biosynthesis regarding isoprenoids and sterols. The activity related to HMGR is regulated through degradation, synthesis, and phosphorylation to keep the level of mevalonate-derived products stable. The human enzyme was successfully targeted through drugs in the clinical

therapy of excessive serum cholesterol levels, along with the physiological regulation of HMGR. The catalytic portion of human HMGR in complexes with HMG-CoA, CoA, and HMG, and HMG, CoA, and NADP (+) can all be seen in three crystal structures, which provide a clear view of the enzyme's active site. The catalytic parts of human HMGR form tetramers. The crystal structure offers a mechanism for cholesterol sensing and indicates how the oligomeric form of the enzyme affects activity. Since bacterial and human HMGRs have different active site architectures, it could be because of this that bacterial HMGRs have not been found to bind HMGR inhibitors. The produced compound [IV] was more effective than the comparative compound [28].

Table 4. Molecular docking of compound [IV]

Docking study					
Compounds	***Binding Energy (PLP Fitness) Kcal/Mol***	***No. of Amino Acids Included in H-bonding***	***Amino Acids Included in H-bonding***	***no. of bonding***	***power of bonding***
1DQ9	66.50	6	ASN 567	1	3.044
			ARG 571	3	2.724 2.807 2.927
			GLU 719	1	2.863
			CYS 561	1	3.044
[IV]	68.00	6	ASN 755	1	2.923
			ARG 568	3	3.011 2.745 2.745
			GLU 559	1	2.887
			SER 865	1	2.838

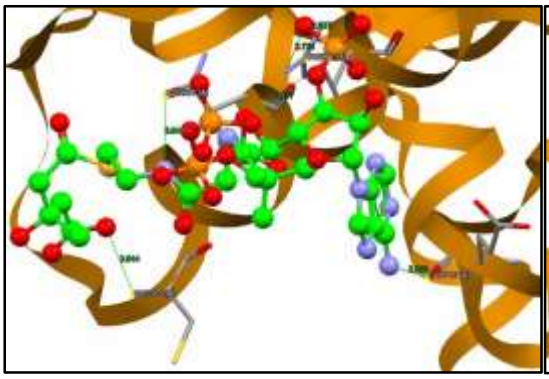

Figure 1. Molecular docking of 1DQ9

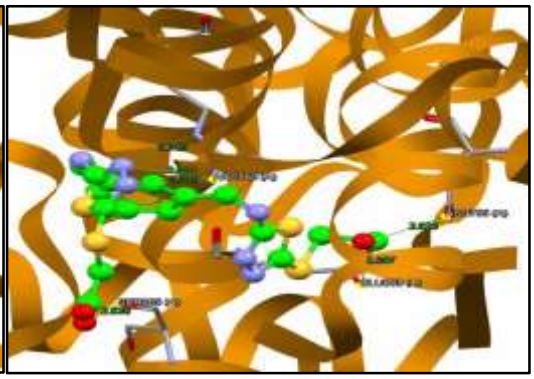

Figure 2. Molecular docking of compound [IV]

3.3 Scanning electron microscope studies (SEM)

The SEM was used to approve the morphology and size of polymers and nanocomposites **Figure (3)** SEM of grafted Chitosan [V], **Figure 4** grafted Chitosan blend with PVA [VII], **Figure 5** nanocomposites of grafted chitosan /PVA /AgNPs [IX]. The average size of Grafted Chitosan particles [V] ranges between (273-312) nm. While the average size of the particles of Grafted Chitosan blends with PVA[VII] is run between (56-78) nm for the presence of PVA, adding PVA results in the alteration of the blend membrane surface topography and has a considerable impact on the cell spreading. The average nano size of the particles ranges between (31- 48) nm for sliver

NPs; AgNPs have been noticed to have homogenous distributions on the matrix surface. The particles in nanocomposite film were found to have almost spherical morphology. However, some of the accumulations of NPs were also found when the surface was rough [29,30].

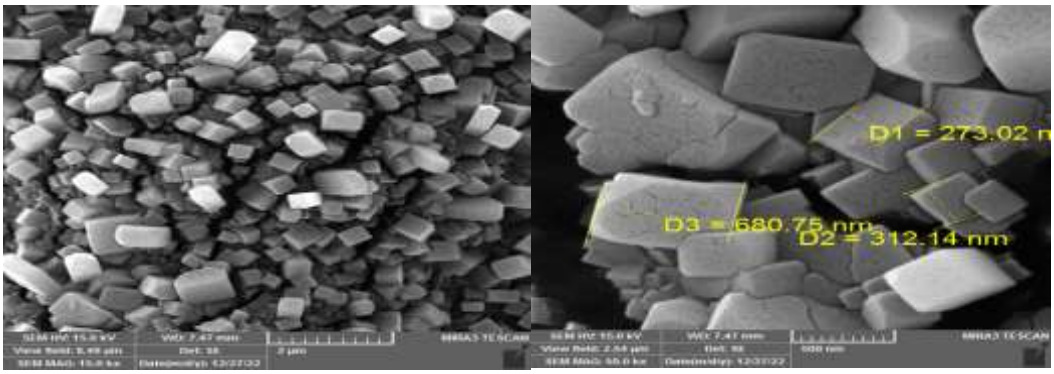

Figure 3. The SEM of Grafted Chitosan [V]

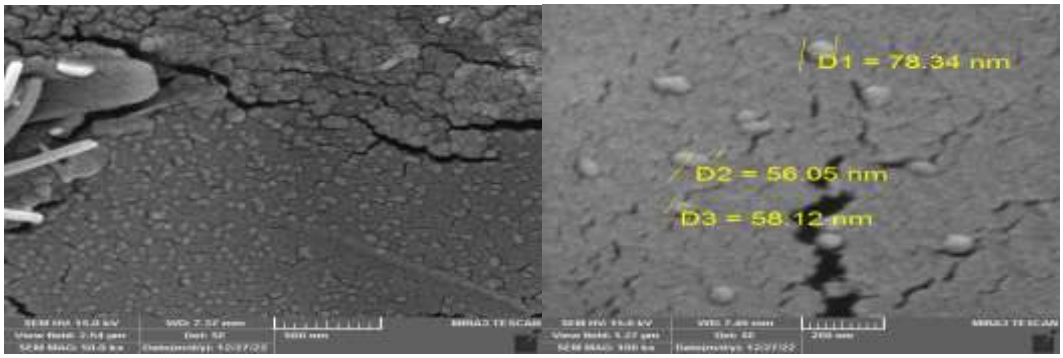

Figure 4. The SEM of Grafted Chitosan / PVA [VII]

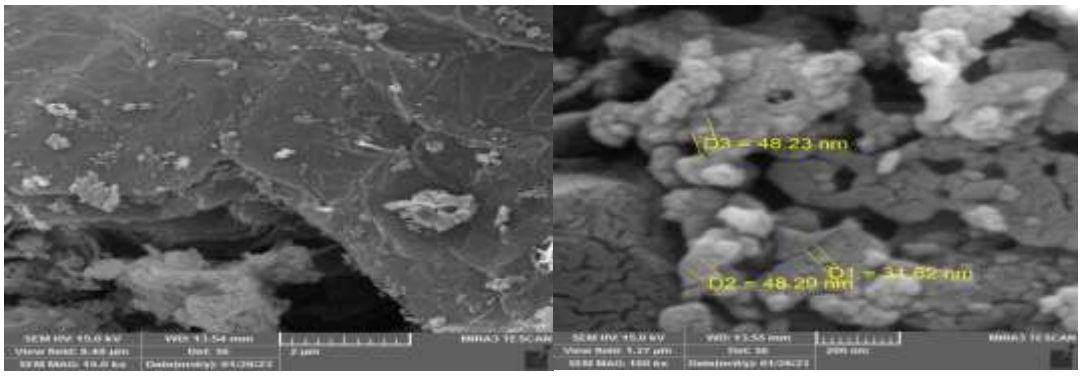

Figure 5. The SEM of polymer Nanocomposities [IX]

3.4 Biological activity

Grafted chitosan, grafted chitosan blended with PVA, grafted chitosan /PVA with gold or silver nanocomposite tested against two pathogenic bacteria types (G+) *Staphylococcus aureus* and *E. coli* (G-) in **Table 5**, and **Figure 6** they all showed excellent inhibition rate, where the nanocomposites were the most activity comparable with Amoxicillin as standard antibiotic. Because of AuNPs' great cell affinity and ease of uptake by immune cells, they can be delivered precisely to the site of infection, where they can inhibit and harm microbial pathogens. The antibacterial effect of silver depends on Ag+, as it binds tightly to electron donor groups in microbial cell walls such as sulfur, nitrogen, or oxygen and enters into the bacterial cell wall, and

the production of free radicals by Ag NPs, which may damage the cell and perforate its membrane [31-35].

Table 5. Antibacterial screening data of some synthesized polymers

Comp.No.	*Escharia .coli*	*Staphylococcus aureus*
Amoxicillin	17	23
[VI]	23	16
[VIII]	25	16
[XI]	30	29
[XII]	27	15

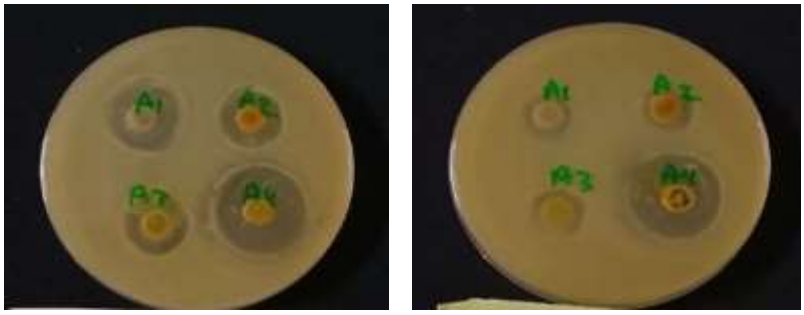

Figure 6. Antibacterial activities of some polymers and nanocomposites

3.5 Anticancer activity

The anticancer activity of various concentrations of some polymers and nanocomposites was investigated against A549 (Human Lung Adenocarcinoma Cells) and REF (R7540) Rat Embryonic Fibroblasts) revealing a good activity, which did not affect the growth of normal Rat Embryonic Fibroblasts. Cell lines were prepared for cytotoxicity assay [36] using cultured cells (96 Wells) in a microtiter plate. The absorbance was measured at (620 nm) on a microplate reader [37]. The cell growth inhibition rate was calculated according to equation [38]:

$$\text{Inhibition rate} = \frac{mean\ of\ control - mean\ of\ treatment}{mean\ of\ control} \times 100$$

The blend polymer [VIII] and nanocomposites [XI, XII] could selectively permeate cancer cells. All polymer nanocomposites [XI, XII] exhibit good inhibition in concentration (100, 50, 25, 12.5) µg/mL more than the polymer blend [VIII] as in **Table 6**. Increasing ROS levels and causing damage to the cellular components by intracellular oxidative stress and an increase in glutathione oxidation AgNPs and AuNPs could induce cytotoxicity [39]. Therefore, the anticancer activity of nanocomposites [XI] (AuNPs) showed significant effects at a concentration of 100 µg/mL against the A549 cell line and IC50=16.92 while IC50=82.68 for REF [40], as in **Table 7** and **Figure7-11**.

Table 6. Inhibition rate of some polymers and naocomposites

Comp.No.	Inhibition rate of L-12.5 µg mL^{-1}	Inhibition rate of 25 µg mL^{-1}	Inhibition rate of 50 µg mL^{-1}	Inhibition rate of 100 µg mL^{-1}
[VIII]	25.12	54.12	55.11	55.98
[XI] =[VIII] +Au	94.64	94.73	95.13	96.23
[XII]=[VIII] +Ag	86..9	87.2	89.34	90.51

Table 7. The IC50 of some polymers and naocomposites

Treatment	IC_{50} in µg/Ml	
	A549	REF
M5 =[VIII]	39.81	72.71
M1=[XI]	16.92	82.68
M3=[XII]	19.41	77.60

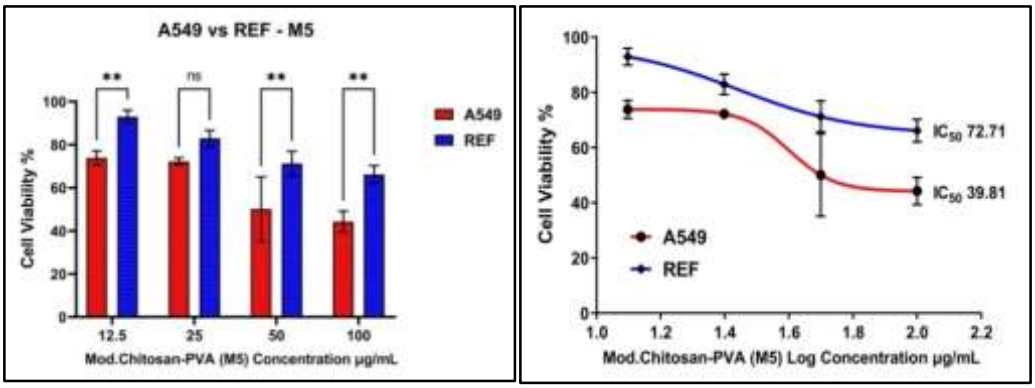

Figure7. The IC50 of M5=[VIII](modified chitosan /PVA)

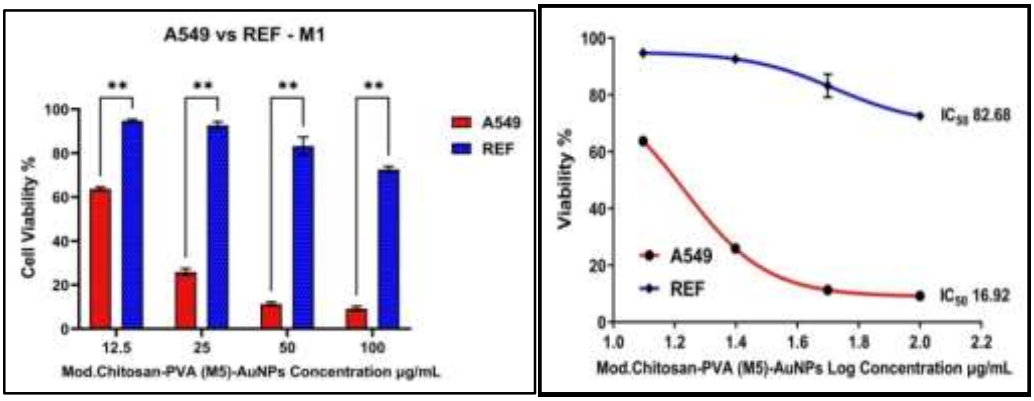

Figure 8. The IC50 of M1=[XI] (modified chitosan /PVA+Au)

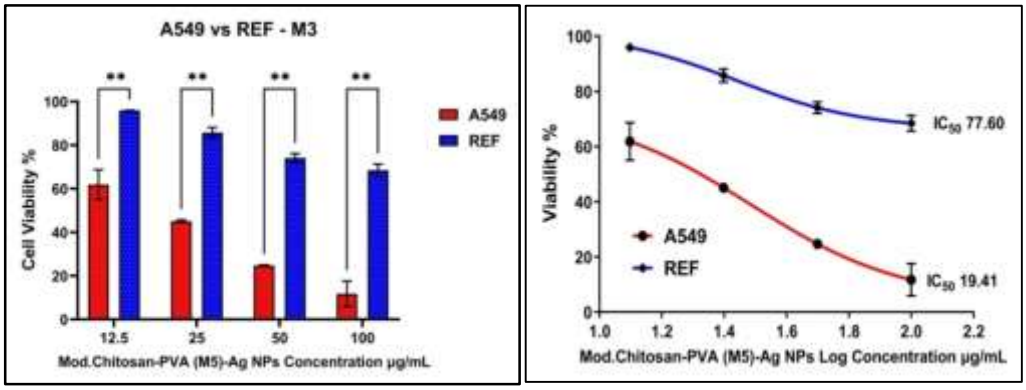

Figure 9: The IC50 of M3=[XII] (modified chitosan /PVA+Ag)

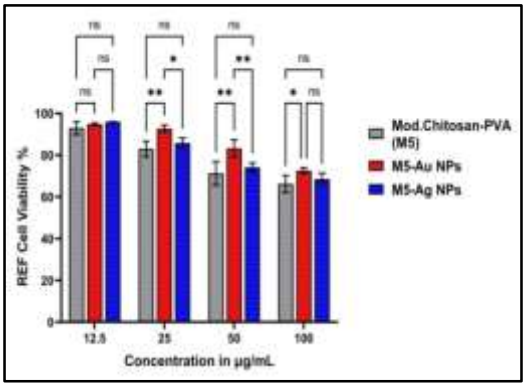

Figure 10. The IC50 of M5 and compare with [M5+Au] and [M5+Ag]

A:Image of well for (A549) before Staining

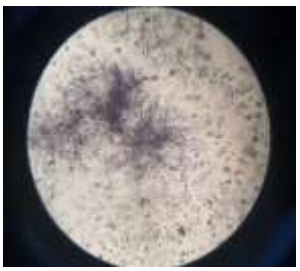

B:Image of well for (A549) after Staining

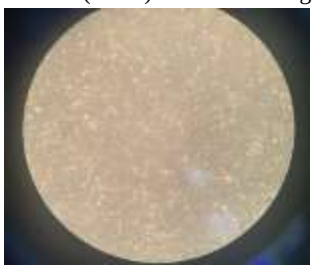

C:Image of well for (REF) before Staining

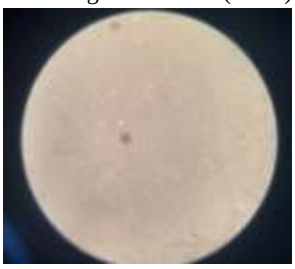

D:Image of well for (REF) after Staining

Figure 11. A: Image of well for (A549) before Staining, **B**:Image of well for (A549) after Staining, **C:**Image of well for (REF) before Staining, and **D:**Image of well for (REF) after Staining

3.6 Study toxicity test

The acute toxicity of some synthesized polymer nanocomposites [XI, XII, XIII) were studied in the Laborator Center for Cancer Research and Medical Genetics according to the Lorke-written method. The study included (25) laboratory mice of the Albino type, with average weights (22-28) gm, three months old, and all males. Mice fasted for 18 hours with free access to water and food before the test. The nanocomposites were dissolved in distilled water and treated through injection. These animals were placed in plastic cages with Metal lids covered with fine sawdust and supplied with water by plastic bottles equipped with food. The treatment group and the control group were compared with doses of the injection, and the study showed after 14 days, no contrast in the weight of the mice daily measured between the group control and the treated groups, and no modification in mice behaviors was carried out, and no toxicity symptoms were reported. Moreover, some mice were sacrificed with cervical dislocation, and kidneys, liver, heart, and lungs were weighed. The visual evaluation of the organs of mice showed normal appearance. These results indicated that polymer nanocomposites have low toxicity towards both investigated organisms [41], as shown on **Figure 12** .

A:Image of mice in plastic cages

B:Image of mice during injection **C**: Image of mice through necropsy

Figure 12. A: Image of mice in plastic cages, **B:**Image of mice during injection, and **C:**Image of mice through necropsy

4. Conclusion

The antibacterial activity of synthesized nanocomposites was evaluated in vitro. The results show that the nanocomposites (grafted chitosan/PVA/AuNPs) exhibited very excellent antimicrobial activities comparable with standard antibiotic as Amoxicillin; MTT assay was used to estimate the cytotoxic effect of different concentrations for cancer cell line (A549) of the created nanocomposites and compare with regular cell line (REF), the (grafted chitosan/ PVA/ Au) exhibited very excellent inhibition rate. Finally, a toxicity test for these nanocomposites was studied, and the results showed these nanocomposites were non-toxic.

Acknowledgment

The authors appreciate the cooperation of the teaching staff in the Department of Chemistry at the College of Education for Pure Science (Ibn Al-Haitham), University of Baghdad**.**

Conflict of Interest

The authors declare that they have no conflicts of interest.

Funding

The research did not receive any financial funding from any institution.

Ethical Clearance

Ethics of scientific research were carried out in accordance with the international conditions followed in dealing with laboratory animals, and included animal health, husbandry and care for it, and providing appropriate conditions for it in terms of food, and appropriate methods were adopted in dealing with it when experimenting, and this is consistent with the instructions of the Iraqi Ministry of Health and Environment.

References

1. Amna, H F.; Samia, A.S.; Yehia, A.B.; Marwa, S.; Elham, M.M.; Mahmoud, A.S. Gold nanoparticles loaded chitosan encapsulate 6-mercaptopurine as a novel nanocomposite for chemo-photothermal therapy on breast cancer. *BMC Chemistry* **2022**, *16*(*94*),1-14. https://doi.org/10.1186/s13065-022-00892-0.
2. Saeed, R.S. Synthesis and characterization of *O*-(carboxyl) chitosan Schiff base derivatives and study antibacterial activity, *Int J Drug Deliv Technol.* **2020**, *10* (*3*), 402- 407. https://doi.org/10.25258/ijddt.10.3.17.
3. Micaela, T.; Elena,T.; Anna,G.; Rosanna,S.; Carmen,S.; Thomas, H.;Susanne, Z.;Alessandro,G. ; Luca, P.; Maria, B. C.; Angela, D.B.; Patrizia, F. Characterization of chitin and chitosan derived from Hermetia illucens, a further step in a circular economy process. *Scientifc Reports* **2022**,*12*(*6613*), 1-17, https://doi.org/10.1038/s41598-022-10423-5.
4. Mohaddeseh, K.; Rezvan, Z.; Azin,K.N.; Reza,M.; Amir, M.M.; Sara, S.; Elham, K.; Nasim, K. Chitosan/polyvinyl alcohol/SiO_2 nanocomposite films: Physicochemical and structural characterization. *Biointerface Res. Appl. Chem* **2022**,*12*(*3*), 3725-3734. https://doi.org/10.33263/BRIAC123.37253734.
5. Paula, S.; Ana, P. L.; Giovanna, M.; Declan,M. D.; Janaina, S. C.; Marcelo, G. Synthesis and characterization of silver nanoparticles for the preparation of chitosan pellet and their application in industrial wastewater disinfection. *Water* **2023**, *15*(*1*),190 , https://doi.org/10.3390/w15010190.
6. Ali, A.T.; Nahida, J.H.; Farah,H.R. Preparation and characterization of (Hyacinth plant / Chitosan) composite as a heavy metal removal. *Baghdad Sci. J.*, **2019**, *16*(*4*) ,865-870. https://doi.org/10.21123/bsj.2019.16.4.0865.
7. Ahmed, A.O.; Gye, H.; Jun, T.K. Antimicrobial, antioxidant, and pH-sensitive polyvinyl alcohol/chitosan-based composite films with aronia extract, cellulose nanocrystals, and grapefruit seed extract . *Int J Biol Macromol.*, **2022** , *213*, 381-393. https://doi.org/10.1016/j.ijbiomac.2022.05.180.
8. Ali, A.T.; Nahida, J. H.; Farah, H. R. Decolorization of phenol red dye by immobilized laccase in chitosan beads using laccase-mediator-system model. *Baghdad Sci. J.*, **2020** *17*(*3*), 720-725. https://doi.org/10.21123/bsj.2020.17.3.0720.
9. Bianca-Elena, B.C.; Loredana,E.N.; Alexandru-Mihail, S.; Alina, G. R.; Florica, D.; Aurica, P.C. New cryogels based on poly(vinyl alcohol) and a copolymacrolactone system: I-synthesis and characterization. *Nanomaterials* **2022**, *12*(*14*),2420, https://doi.org/10.3390/nano12142420.
10. Hitesh,C.; Shabana, B.; Sandeep,K.; Muhammad, S. K. ; Pradeep, K.; Inderbir, S. Preparation and evaluation of chitosan/PVA based hydrogel films loaded with honey for wound Healing application. *Gels* **2022**, *8*(*2*) ,111. https://doi.org/10.3390/gels8020111.
11. Duaa, A.; Nahida, J. H. Preparation and characterization of PANI/PVA blends as electrolyte materials. *Journal of Applied Sciences and Nanotechnology* **2022**, *2*(*2*),38-46. https://doi.org/10.53293/jasn.2022.4124.1073.
12. Diana, S.; Tăchită ,VB.; Mihaela , D. O.;Florica, D. ; Corneliu , H.; Alina-Mirela , I.; Alexandru, A.; Gabriela, L.; Ion, A.;Ioana, Emilia¸S. ; Vasilica , P. Phosphorylated poly(vinyl alcohol) electrospun mats for protective equipment applications. *Nanomaterials* **2022**,*12*(*15*),2685. https://doi.org/10.3390/nano12152685.

13. Baodong, L.; Jianhua, Z.; Hongge , G. Research progress of polyvinyl alcohol water-resistant film materials. *Membranes* **2022**,*12*(*3*),347. https://doi.org/10.3390/membranes12030347.
14. Hongyu, X.;Ying, S.; Li G.;Nan, S.; Junyan , Y.; Rui, H. Preparation and characterization of PH-responsive polyvinyl alcohol/chitosan/ anthocyanin films , *Food Sci. Technol Campinas* **2023**, *43*(e98022),1-12 https://doi.org/10.1590/fst.98022.
15. Mohamed, A. E.; Taha ,A.H.; Mamdouh, M.S. Polyvinyl alcohol/gum Arabic hydrogel preparation and cytotoxicity for wound healing improvement. *e-Polymers* **2022**,*22*, 566–576. https://doi.org/10.1515/epoly-2022-0052.
16. Leandro A. A.; Bruno, V. M. R.; Debora, T. B.; Rafael, S.; Luiza, A. M.; Amanda, F. F.; Adrian, P. Chitosan/gold nanoparticles nanocomposite film for bisphenol A electrochemical sensing . *Electrochem* **2022**, *3*, 239-247. https://doi.org/10.3390/electrochem3020016.
17. Marco, L.M.; Jeanne, P. L.; Lyka, B. D. ; Mikee, J. D. ; Jonathan, N. P.; Ser, J. L.; Susan, D. A.; Jonathan, P. M.; Eleanor, S. A.; Arnold ,C.A.; Custer, C. D.; Rey,Y. C. Preparation of spin-coated poly(vinyl alcohol)/ chitosan/ gold nanoparticles composite and its potential for colorimetric detection of cyanide in water. *Pol. J. Environ. Stud.*, **2022** , *31*(*2*), 1569-1576. https://doi: 10.15244/pjoes/140276.
18. Zhijun, G.; Dan, S. ; Xian, Z.; Huan, X.; Yizhou, H.; Chenglin, C.; Baolong,S. AuNP/chitosan nanocomposites synthesized through plasma induced liquid chemistry and their applications in photothermal induced bacteria eradication. *Pharmaceutics* **2022**, *14*(*10*), 2147. https://doi.org/10.3390/pharmaceutics14102147.
19. Amr, H.H.; Amr, M.S.; Omar, M.A.; Salem, S.S. Synthesis of chitosan- based gold nanoparticles : antimicrobial and wound-healing activities, *Polymers* **2022**,*14*(*11*), 2293. https://doi.org/10.3390/polym14112293.
20. Danmin, Y. ; Qun, L.; Yahui, G.; Shoumei, W.; Fanrong, M.; Wuyin, W.; Yucang, Z. Characterization of silver nanoparticles loaded chitosan/polyvinyl alcohol antibacterial films for food packaging. *Food Hydrocolloids* **2023**, *136*, Part B, 108305. https://doi.org/10.1016/j.foodhyd.2022.108305.
21. Ali, H.S.; Khalid, F.A.; Ruwaidah S.S. Synthesis and characterization of some new thiazine, azetidine and thiazolidine compounds containing 1,3,4- thiadiazole moiety and their antibacterial study, *Ibn Al-Haitham Jour. for Pure & Appl. Sci.*, **2014** ,*27* (*3*),350-364. https://jih.uobaghdad.edu.iq/index.php/j/article/view/302.
22. Saeed, R.S.; AL-Rawi, M.S. Synthesis, characterization, study the toxicity and anticancer activity of *N*,*O*-Chitosan derivatives. *International Journal of Pharmaceutical Research* **2020**, *12*(*2*), 1197-1206. https://doi.org/10.31838/ijpr/2020.12.02.0180.
23. Samir, A.H.; Saeed, R.S; Matty, F.S. Synthesis and study of modified polyvinyl alcohol containing amino acid moieties as anticancer agent, *Oriental Journal of Chemistry*, *2018*, 34(*1*), 286-294. http://dx.doi.org/10.13005/ojc/340131.
24. Zhimei, Z.; Bayaer, A.; Hui, X.; Shuang, Z. Structure and antimicrobial activities of benzoyl phenyl-thiosemicarbazonechitosans. *International Journal of Biological Macromolecules* **2012** ,*50* ,1169-1174. https://doi.org/10.1016/j.ijbiomac.2012.01.004.
25. Li, X.; Goh, S.H.; Lai, Y.H.; Wee, A.T. Miscibility of carboxyl-containing polysiloxane/ poly(vinylpyridine) blends. *Polymer* **2000**, *41*(*17*), 6563-6571. https://doi.org/10.1016/S0032-3861(99)00896-4
26. Hafeez, H.Y.; Lakhera, S.K.; Ashokkumar, M.; Neppolian, B. Ultrasound assisted synthesis of reduced graphene oxide (rGO) supported $InVO_4$-TiO_2 nanocomposite for efficient hydrogen

production. *Ultrason Sonochem*. **2019**, *53*, 1-10. https://doi.org/10.1016/j.ultsonch.2018.12.009.

27. Badawy, M.E.I.; Rabea, E.I. Preparation and antimicrobial activity of O-(benzoyl) chitosan derivatives against some plant pathogens. *African Journal of Microbiology Research* **2013**, *7*(*20*) , 2259- 2268. https://doi.org/10.5897/AJMR12.1185.
28. Eva, S.I.; , Maya, P.; Susan, K.B.; Johann, D. Crystal structure of the catalytic portion of human HMG-CoA reductase: insights into regulation of activity and catalysis .The *EMBO Journal* **2000**, *19* (*5*),819-830. https://doi.org/10.1093/emboj/19.5.819.
29. Parul, S.; Garima, M.; Navendu, G.; Sanjeev, K.S.; Sanjay, R.D. Evaluating the potential of chitosan/poly(vinyl alcohol) membranes as alternative carrier material for proliferation of Vero cells .*e-Polymers* **2015**, *15*(*4*), 237-243. https://doi.org/10.1515/epoly-2015-0021.
30. Mohammed, A.A.; Mazin, N.M.; Mohammed, S. Chemical modification and characterization of chitosan for pharmaceutical applications. *Egypt. J. Chem*. **2021**, *64*(*7*), 3635-3649. https://doi.org/10.21608/ejchem.2021.61809.3331.
31. Omnia, M.; Abdallah, K. Z.;Mostafa, M. H.; Mervat, I.; Gamal, A. Antibacterial, antibiofilm and cytotoxic activities of biogenic polyvinyl alcohol-silver and chitosan-silver nanocomposites . *Journal of Polymer Research* **2020**, *27*(*3*),74. https://doi.org/10.1007/s10965-020-02050-3.
32. Amdadul, H.; Ashra, F.; Anowar, K.; Renukadevi, B.; Mizanur, R.; Hyung, K.; Shahina, A. Chitosan-coated polymeric silver and gold nanoparticles: Biosynthesis, characterization and potential antibacterial applications: A Review. *Polymers* **2022**, *14*(*23*),5302. https://doi.org/10.3390/polym14235302.
33. Kokila,T.; Chaitany, J. R.; Vanaraj, R.; Selvakumari, U.; Madhappan S.; Vinit, R.; Gopal S. K.;Thi,T.V.; Seong, K. Update on chitosan-based hydrogels: Preparation, characterization, and its antimicrobial and antibiofilm applications. *Gels*, **2023**, *9*(*1*),35. https://doi.org/10.3390/gels9010035.
34. Nebras M. Jamel, Rajaa K. Baker, Jumbad H. Tomma, Synthesis, characterization and investigation the antibacterial activity of new heterocyclic compounds derived from 4-(4`-methoxy benzoyloxy) benzaldehydethiosemicarbazone, *Ibn Al-Haitham Jour. for Pure & Appl. Sci.*, **2017**,*30* (*1*), 155-168. https://jih.uobaghdad.edu.iq/index.php/j/article/view/1068/916.
35. Saeed, R.S.; Matty, F.S.; Samir, A.H. Al-Rawi, M.S. Synthesis, characterization and antibacterial study of selected metal complexes derived from modified of PVA, *Int J Drug Deliv Technol.*, **2019**, *11*(02 Suppl.):108-117.
36. Freshney, RI. Culture of animal cells: A manual of basic technique and specialized applications; Ed.; 6th , Wiley: New York ,**2010**. https://doi.org/10.1002/9780470649367.
37. AL-Rawi, M.S.; Hassan, H.A; Hassan, D.F. Synthesis, anti-bacterial and anti-cancer activities of some antipyrine diazenyl benzaldehyde derivatives and antipyrine based heterocycles . *Iraqi National Journal of Chemistry* **2017**, *17* (*2*),140-148 https://www.iasj.net/iasj/article/186761.
38. Gao, S.; Ya, BP. ; Dong, WG.; Luo, HS. Ant proliferative effect of octreotide on gastric cancer cells mediated by inhibition of Akt/PKB and telomerase, *World J. Gastroenterology* **2003**, *9* (10) , 2362- 2365. https://doi.org/10.3748/wjg.v9.i10.2362.

39. Ekaterina,O.M. Gold nanoparticles: Biosynthesis and potential of biomedical application. *J. Funct. Biomater* **2021**,*12*(*4*), 70. https://doi.org/10.3390/jfb12040070.
40. Mohammadreza, A.; Masoumeh, M.C.; Alireza, H.; Negar, F.; Zahra, K.; Parastoo, F.; Fardad, F.; Kasra, M.B.; Hassan, N.; Ebrahim, M. Polyvinyl alcohol (PVA)-based nanoniosome for enhanced in vitro delivery and anticancer activity of thymol, *Int J Nanomedicine.* **2023**, *18*,3459-3488. https://doi.org/10.2147%2FIJN.S401725.
41. Ake-Assi, E.; N'guessan, K.; Kouassi, A.F. Evaluation de la toxicite aigue de l'extrait aqeux des feuilles de thunbergia atacorensis, une espece nouvell. *European Scientific Journal*, **2015**,*11* (*27*), 92- 100. https://eujournal.org/index.php/esj/article/view/6261.